Prestack considerations for the migration of oblique reflectors

John C. Bancroft and Charles P. Ursenbach

ABSTRACT

A zero-offset stacked section that contains an oblique reflector can be migrated successfully by raising the migration velocity. What prestack processing can be performed to improve the diffracted energy on the stacked section?

A special moveout correction can be applied to enhance the oblique reflection on the stacked section and modified prestack migration operators may also be used to enhance the oblique reflection. The benefit of these special processes will depend on the linear extent and angle of the oblique reflector. Satisfactory results can also be obtained when stacking with the RMS velocity and when stacking with an RMS velocity that is increased by the inverse of the cosine of the angle of obliquity.

INTRODUCTION

A special 2-D poststack migration of oblique reflectors was described by French (1975) in which the migration velocity V_{mig} is increased over the RMS velocity V_{rms} as given in equation (1)

$$V_{mig} = \frac{V_{rms}}{\cos\gamma}, \tag{1}$$

where γ is the angle of obliquity, as illustrated in Figure 1.

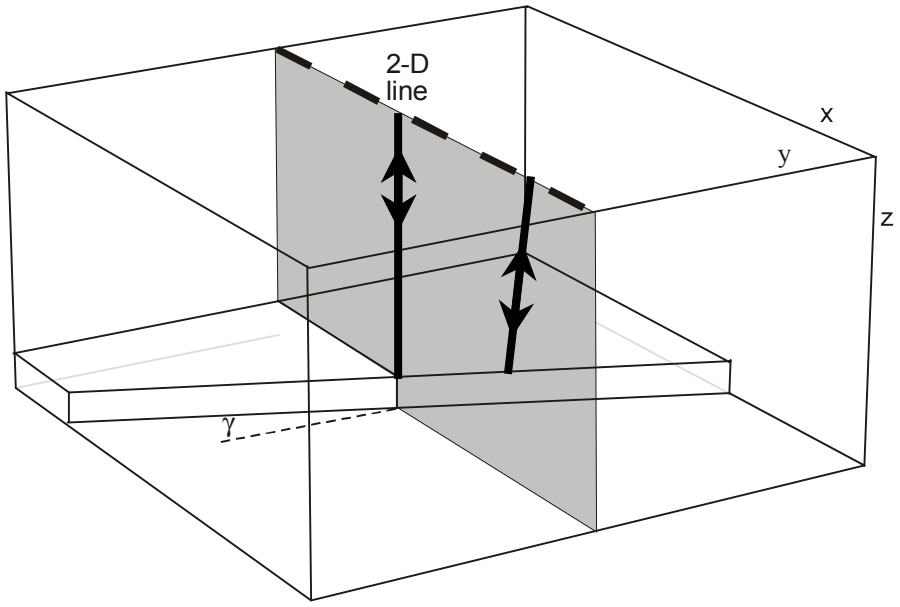

Figure 1. A perspective view of a 2-D seismic line above an oblique reflector.

It is assumed that the medium below the seismic line is horizontally layered and that travel times may be estimated using RMS velocities.

Figure 2 is a plan view of Figure 1, and illustrates the zero offset raypaths for different surface locations. The raypaths are confined to vertical planes that are normal to the oblique reflector. The reflection points on the reflector move away from the vertical plane of the seismic line to maintain a normal reflection (required by zero offset) and to find the minimum traveltime (a condition of Fermat's principle).

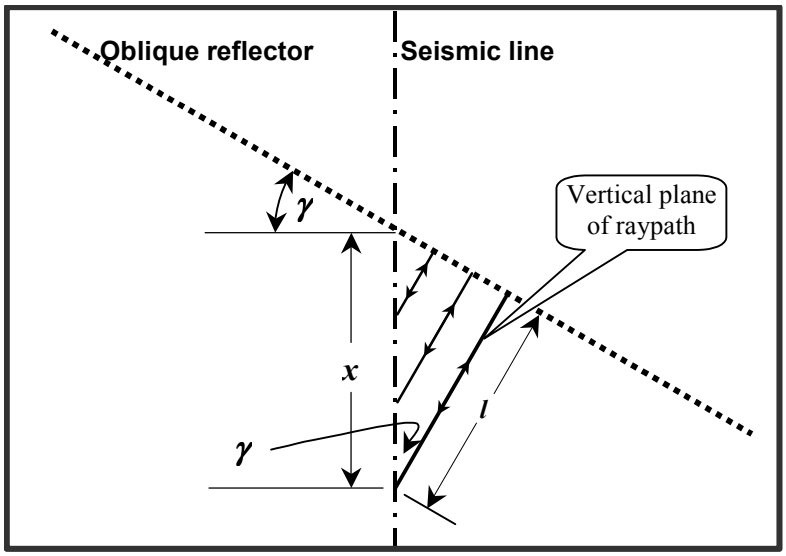

Figure 2. Plan view of an oblique reflector showing zero-offset raypaths that are confined to vertical planes.

If the angle of obliquity were zero, then all reflections would occur on the reflector below the vertical plane of the seismic line. Consequently, the reflection point will behave as a conventional scatterpoint and produce the conventional shape of a diffraction, defined in time migration as

$$T^2 = T_0^2 + \frac{4x^2}{V_{rms}^2} \quad , \tag{2}$$

where T is the two-way traveltime, T_0 the vertical two-way traveltime from the reflector, and x the horizontal distance from the scatterpoint to the colocated source and receiver.

When the angle of obliquity is not zero, the reflection point moves away from the seismic line, and the horizontal distance l from the reflection point to the colocated source and receiver becomes

$$l = x\cos\gamma \quad , \tag{3}$$

giving a new diffraction shape defined by

$$T^2 = T_0^2 + \frac{4x^2 \cos^2 \gamma}{V_{rms}^2} \quad , \tag{4}$$

the equation described by French (1975), and gives the migration velocity defined by equation (1).

The migration of oblique reflectors is not obvious when processing data as the geometry of the subsurface is usually not known. If it appears that a portion of the migrated section is under-migrated (i.e. the appearance of un-collapsed diffractions), then a number of migrated sections may be produced, each formed with an increase in the percentage of the RMS velocity. The process of migrating with increased velocities continues until a satisfactory migrated image is obtained. Software has been developed in which a small window (porthole) around the area of interest may be migrated in real time by sliding a velocity bar. Once the optimum migrated image has been obtained, the RMS and migrated velocities can be used to estimate the magnitude of γ, the angle obliquity. The actual sign of the angle is not determined, but a number of 2-D lines in the area may then be used to map these angles to estimate the location of the oblique reflector. This method has been used successfully to map channel sands and faults. In one processing case, a difficult area of a section with an apparent cycle skip, was migrated with a velocity of $3*V_{rms}$, to produce a clear image of a fault, with an angle of obliquity of approximately 70 degrees.

Figure 3 shows two migrations at 100% and 130% of the RMS velocities, where the RMS velocities were estimated using a DMO process. The 100% image appears acceptable, however, when examining the 130% image, a fault (γ = 40 degrees) becomes evident in the center of the section.

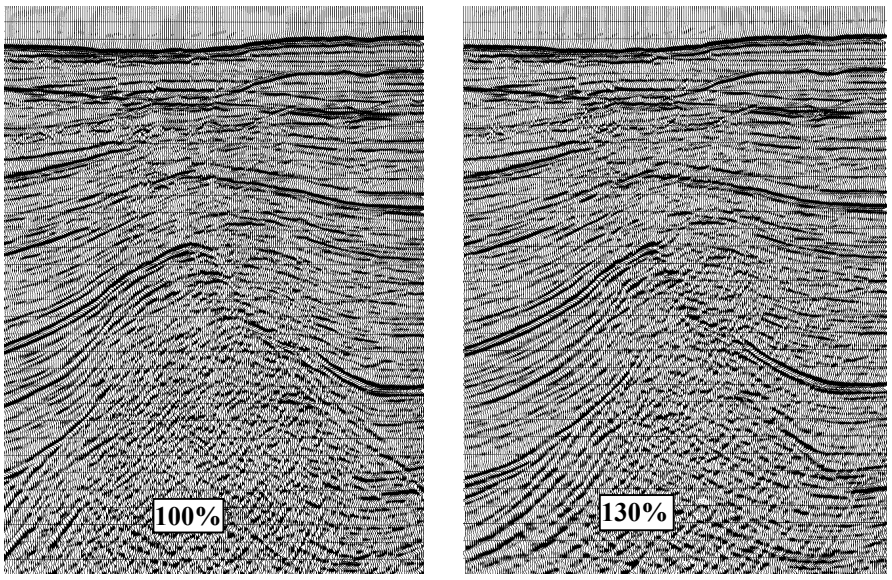

a) b)

Figure 3. Two migrated images, a) with 100% V_{rms} and b) 130% V_{rms}.

Note that modifying the migration velocities to image oblique reflections is only valid for that part of the section that contains the oblique reflections. Other parts of the section will be over migrated. A final migrated section may be formed with a cut and paste method that includes the oblique images with the original migration.

The above discussion has been confined to stacked data that tends to approximate a zero-offset section. The zero-offset approximations break down when the reflectors are dipping and or when the reflectors are oblique to the 2-D line. The following discussion evaluates the shape of a *prestack* reflection from a horizontal oblique reflector, then evaluates the results of stacking for a poststack migration and formulates options for prestack migration.

PRESTACK CONSIDERATIONS OF OBLIQUE REFLECTORS

Consider a plan view of the oblique reflecting surface in Figure 4. Note the location ***A*** where the seismic line and the oblique reflector intersect. The CMP gather at ***A*** contains source-receiver locations identified by the square braces. All raypaths will be symmetrical in the vertical plane below the seismic line with a reflector point that is located below ***A***. The moveout on the offset traces will appear to have a scatterpoint at ***A***, and have the RMS velocities associated with an orthogonal reflector.

Reflections from a CMP gather located at ***B*** will be considerably different from the reflections at ***A***. At ***B,*** the zero offset reflection has a migration velocity V_{mig} defined in equation (1). Small offsets from B will have a reflection point that is very close to the zero offset point and will therefore have a geometry that is similar to zero offset and will have a moveout velocity close to V_{mig}. For larger offsets, the reflector point will move along the reflector towards A. The location of the reflection point was difficult to define and will be described in an appendix.

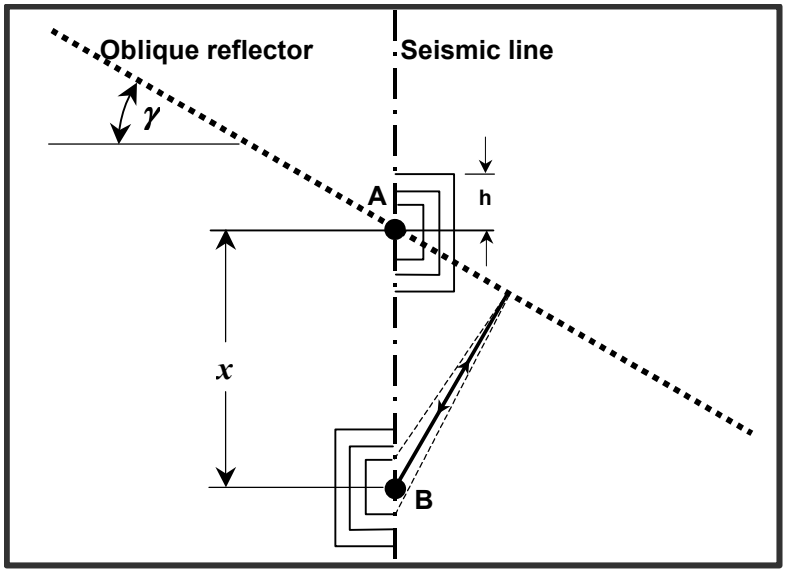

Figure 4. Plan view of an oblique reflector showing zero-offset raypaths that are confined to vertical planes.

The prestack traveltime surface of reflections from an oblique reflector for CMP locations x and offsets defined by h is defined by equation (A10) of the appendix and is shown in Figure 5a. This shape is similar to a Cheops pyramid (Figure 5b) for a scatterpoint at $\boldsymbol{A}$ (or a normal reflector). Figure 5c contains a plot of both surfaces for comparison. The prestack travel time surface defined by equation (A10) is the summation surface required for a prestack Kirchhoff migration.

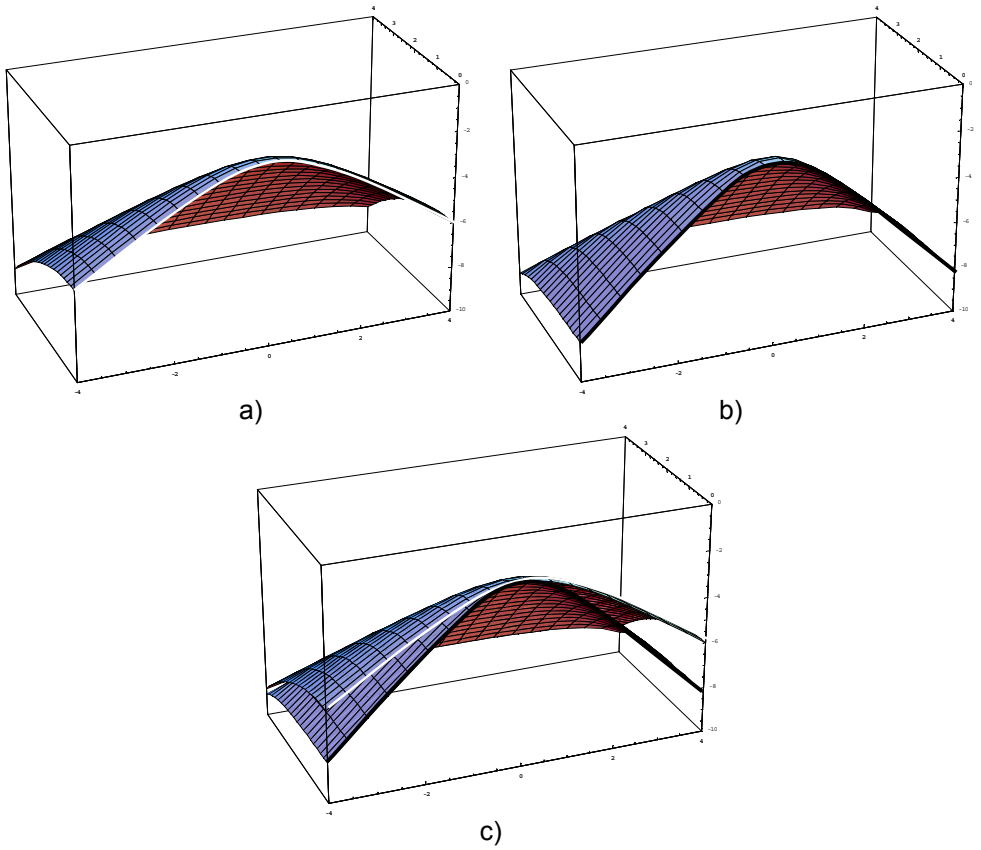

Figure 5. Prestack traveltime surface of a) an oblique reflector, b) Cheops pyramid, and c) a combined display.

Note in Figure 5c the difference in the zero offset hyperbolas defined by V_{rms} for the scatterpoint, and V_{mig} for the oblique reflector. It may also be assumed that the offset curvature through the peak are the same and have a moveout velocity V_{rms}. The moveout with maximum displacement x can be observed at the left side of the figure. Note the Cheops pyramid moveout is quite flat (near zero offset) and requires a moveout velocity that is modified by the corresponding dip on the zero offset diffraction. The moveout on the oblique reflector surface (ORS) appears more hyperbolic with a lower velocity. Many attempts were made to approximate the ORS including a Taylor series expansion about h. Some of these results are contained in the appendix, but the two simplest surfaces, using stacking velocities of V_{rms} and $V_{rms}/cos(\gamma)$ are shown below in Figure 6.

Figure 6a shows the stacking surface of conventional processing that uses V_{rms} for conventional NMO correction (along with the defined ORS identified with the arrow). This surface is defined by equation (5),

$$T^2 = T_0^2 + \frac{4x^2 \cos^2 \gamma}{V_{rms}^2} + \frac{4h^2}{V_{rms}^2} \quad . \tag{5}$$

The first two terms on the right-hand side of equation (5) that involve T_0 and x define the zero-offset time as a function of x. The third term involving h is the conventional moveout term. Note the curvature on the left side of Figure 6a is too low.

Equation (6) uses the oblique angle γ to modify the moveout velocity and is shown in Figure 7b.

$$T^2 = T_0^2 + \frac{4x^2 \cos^2 \gamma}{V_{rms}^2} + \frac{4h^2 \cos^2 \gamma}{V_{rms}^2} \quad . \tag{6}$$

Now the velocity match on the left side of Figure 6b is much better as predicted earlier. However, when the back of Figure 6b is viewed in Figure 6d, the zero displacement velocity (x=0) is in error.

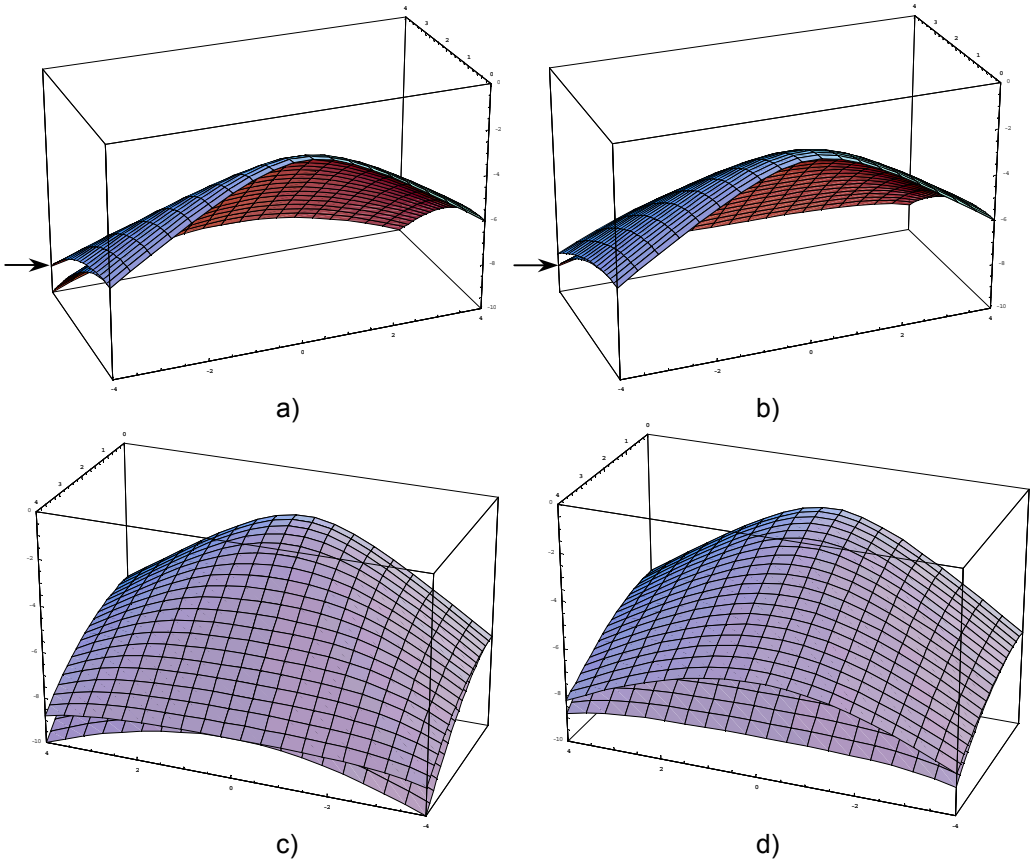

Figure 6. Combined plots of the oblique reflector surface with a) conventional moveout, and b) with moveout velocities using V_{mig} defined in equation (1). The rear view of (a) and (b) are shown in parts (c) and (d) respectively.

COMMENTS AND CONCLUSIONS

1. Prestack migration of oblique reflectors can be accomplished with a summation surface defined by equation (A10) and converted to time using the RMS velocity.

2. The maximum offset used in the figures assumes an offset h four times the depth of the reflector. This offset is quite large for conventional processing. Typical processing may limit the offsets to be comparable to the depth of the reflector. The maximum migration displacement x is also quite large and corresponds to migration dips up to 75 degrees.

3. Stacking oblique reflection data with conventional moveout velocities V_{rms} will produce a diffraction that is only focussed near the apex. The larger displacements (x) of the diffraction will not be focussed.

4. Use of a stacking velocity V_{mig} that is modified for the obliquity reflector will produce a diffraction that is focussed on the flanks of the diffraction, but will not focus at the apex.

5. The above discussion has assumed that the oblique reflector is linear, possibly from a fault. However, if the reflector is not linear, such as that from a buried river channel, then only that part of the reflector close to the seismic line (or small offsets) should be used. In this case, use of the conventional V_{rms} velocities may produce the best overall stack of the diffraction.

6. More complex moveout functions, based on a Taylor series approximation to the oblique reflecting surface may be useful if small offsets of h are used (see appendix).

REFERENCES

French, W. S., 1975, Computer migration of oblique seismic reflection profiles, Geophysics, 40. 961-980

APPENDIX

The math for deriving the travel times from an oblique reflector is derived in this appendix. A number of approaches were taken based on the physical geometry of the problem. The only method that was successful was using Fermat's principle that reduces to the raypath with minimum travel time. The subsurface model used assumed a constant velocity of unity (V = 1) allowing the traveltimes to be estimated as distance. The depth of the scatterpoint was located at a depth z = 1, with the maximum displacement and offset of x = h = 4. The source location is defined by $(x_s, y_s = 0, z_s = 0)$, the receiver location by $(x_r, y_r = 0, z_r = 0)$, the reflection point on the oblique line (x, y, z), the angle of obliquity γ, and the relative slope of the reflector in the x-y plane is $m=\tan(\gamma-\pi/2)$.

Given a source location defined by the displacement x_s, and the offset h, the length of raypath l_s to any point (x, y) on the oblique reflector is defined by equation (A1).

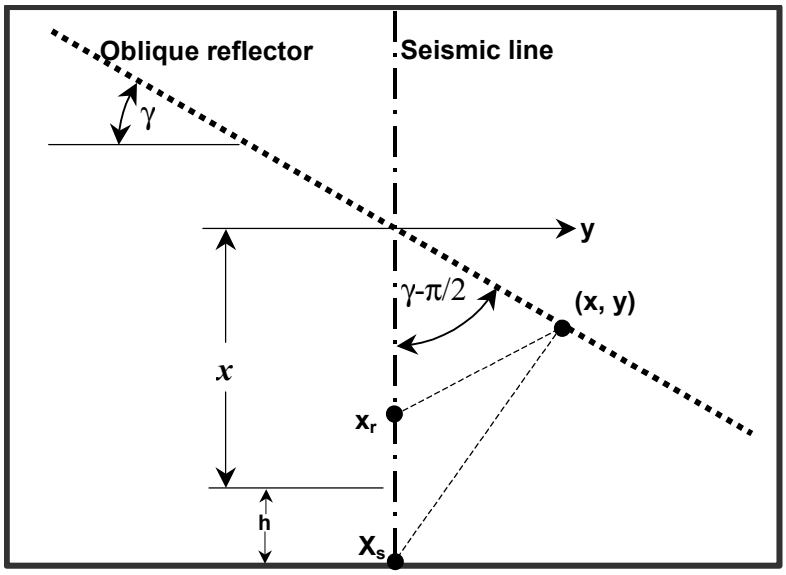

Figure A1. Plan view of an oblique reflector showing offset raypaths.

$$l_s = \left[(x_s - x)^2 + y^2 + z^2\right]^{1/2}, \tag{A1}$$

and the length of the receiver ray l_r is

$$l_r = \left[(x_r - x)^2 + y^2 + z^2\right]^{1/2}. \tag{A2}$$

The total length of the raypath l combines equations (A1) and (A2) to give the double square-root equation (A3),

$$l = \left[(x_s - x)^2 + y^2 + z^2\right]^{1/2} + \left[(x_r - x)^2 + y^2 + z^2\right]^{1/2} . \quad \text{(A3)}$$

Converting the y parameter in (A3) to x using the linear equation $y = mx$ we get

$$l = \left[(x_s - x)^2 + m^2x^2 + z^2\right]^{1/2} + \left[(x_r - x)^2 + m^2x^2 + z^2\right]^{1/2} . \quad \text{(A4)}$$

Taking the derivative of equation (A3) with respect to x and equating it to zero will define a value for x that gives the minimum length of the raypath. i.e.

$$\frac{dl}{dx} = \frac{d\left\{\left[(x_s - x)^2 + m^2x^2 + z^2\right]^{1/2} + \left[(x_r - x)^2 + m^2x^2 + z^2\right]^{1/2}\right\}}{dx} . \quad \text{(A5)}$$

$$\frac{dl}{dx} = \frac{2m^2x - 2(x_s - x)}{2\sqrt{m^2x^2 + (x_r - x)^2 + z^2}} + \frac{2m^2x - 2(x_r - x)}{2\sqrt{m^2x^2 + (x_s - x)^2 + z^2}} = 0 . \quad \text{(A6)}$$

Solving this equation for x was difficult and MATHEMATICA was also unable to obtain a solution with the equation in this form. The expression was put in the form

$$\frac{2m^2x - 2(x_s - x)}{2\sqrt{m^2x^2 + (x_r - x)^2 + z^2}} = -\frac{2m^2x - 2(x_r - x)}{2\sqrt{m^2x^2 + (x_s - x)^2 + z^2}} . \quad \text{(A7)}$$

and each side squared so that it could then be rearranged to a quadratic function in x.

$$m^2(1+m^2)(x_r + x_s)x^2 + 2[(1+m^2)z^2 - x_r x_s]x - (x_r + x_s)z^2 = 0 . \quad \text{(A8)}$$

Solving this gives two solutions, only one of which is correct. (An invalid solution is introduced by squaring equation (A7).) The correct solution for x is

$$x = \frac{m^2x_r x_s - (1+m^2)z^2 + \sqrt{m^2x_r^2 + (1+m^2)z^2}\sqrt{m^2x_s^2 + (1+m^2)z^2}}{m^2(1+m^2)(x_s + x_r)} . \quad \text{(A9)}$$

The value for y is obtained from the linear equation $y = mx$. Now the reflection point *(x, y, z)* is defined, and the value of x is then inserted into equation (A4) to give the length of the raypath. This yields an expression for $l = l(m,z,x_r,x_s)$. A new expression for l is then obtained by substituting $x_s = x + h$ and $x_r = x - h$, where x is now understood to be the offset (see the two definitions of x in Figure A1). This results in the following expression:

$$l = \frac{1}{m^2x\sqrt{2(1+m^2)}}\left[\sqrt{(1+m^2)z^2 + m^2(h-x)^2} + \sqrt{(1+m^2)z^2 + m^2(h+x)^2}\right]$$
$$\times\sqrt{2m^4x^2 + (1+m^2)z^2 + m^2(h^2+x^2) - \sqrt{(1+m^2)z^2 + m^2(h-x)^2}\sqrt{(1+m^2)z^2 + m^2(h+x)^2}} \quad \text{(A10)}$$

A number of attempts were initiated to simplify this equation. One of the more successful attempts was using MATHEMATICA to express $l = l(m,z,x,h)$ as a power series in h. Simplifying the result into a 4th order approximation gave the following result:

$$\text{length} = 2\sqrt{\frac{m^2 x^2}{1+m^2} + z^2} + h^2 \frac{\sqrt{\frac{m^2 x^2}{1+m^2} + z^2}\left(m^2 x^2 + (1+m^2)^2 z^2\right)}{\left(z^2 + m^2 (x^2 + z^2)\right)^2} - h^4 \frac{\sqrt{\frac{m^2 x^2}{1+m^2} + z^2}\left(m^4 x^4 - 2 m^2 (-1 - 2 m^2 + m^4 + 2 m^6) x^2 z^2 + (1+m^2)^4 z^4\right)}{4 \left(z^2 + m^2 (x^2 + z^2)\right)^4} \tag{A11}$$

The 2nd order approximation from the above equation (A11) is plotted in Figure A2.

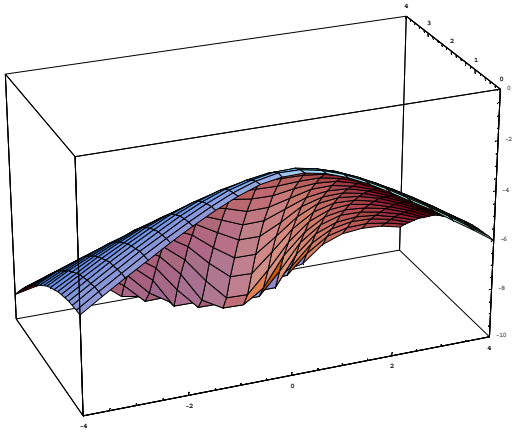

Figure A2. Surface plot of 2nd order Taylor series expansion from equation (A10).

The surface displayed in Figure A2 is definitely inferior to the simple surfaces using conventional NMO correction with V_{rms} and V_{mig}. It should be noted that the initial MATHEMATICA Taylor series expansion filled approximately 30 pages. Odd order terms would eventually simplify to zero, and the even order terms simplified to those given above.